gibco

24 days of stem cells

Shape the future of stem cell innovation

October 1- November 1, 2019

Join us for 24 Days of Stem Cells; a premiere virtual event featuring the latest advances in stem cell research.

This year's format will feature a new hour of cutting edge content every week day starting October 1st. Attend the sessions that are most relevant to your work - at your convenience and at your pace.

During the 24-day long event, you can:

- Access leading scientific presentations from thought leaders around the world
- Watch live training demonstrations from our stem cell experts
- Download key stem cell tools and resources
- Complete weekly challenges to earn points towards certification and prizes

Register today at
www.24daysofstemcells.com

ThermoFisher SCIENTIFIC

WILEY

Journal of Neuroscience Research

Journal of Neuroscience Research 88:1433–1444 (2010)

Functional Silica Nanoparticle-Mediated Neuronal Membrane Sealing Following Traumatic Spinal Cord Injury

Youngnam Cho,[1] Riyi Shi,[1,2] Albena Ivanisevic,[2,3] and Richard Ben Borgens[1,2]*

[1]Center for Paralysis Research, School of Veterinary Medicine, Purdue University, West Lafayette, Indiana
[2]Weldon School of Biomedical Engineering, Purdue University, West Lafayette, Indiana
[3]Department of Chemistry, Purdue University, West Lafayette, Indiana

The mechanical damage to neurons and their processes induced by spinal cord injury (SCI) causes a progressive cascade of pathophysiological events beginning with the derangement of ionic equilibrium and collapse of membrane permeability. This leads to a cumulative deterioration of neurons, axons, and the tissue architecture of the cord. We have previously shown that the application of the hydrophilic polymer polyethylene glycol (PEG) following spinal cord or brain injury can rapidly restore membrane integrity, reduce oxidative stress, restore impaired axonal conductivity, and mediate functional recovery in rats, guinea pigs, and dogs. However there are limits to both the concentration and the molecular weight of the application that do not permit the broadest recovery across an injured animal population. In this study, PEG-decorated silica nanoparticles (PSiNPs) sealed cells, as shown by the significantly reduced leakage of lactate dehydrogenase from damaged cells compared with uncoated particles or PEG alone. Further in vivo tests showed that PSiNPs also significantly reduced the formation of reactive oxygen species and the process of lipid peroxidation of the membrane. Fabrication of PSiNPs containing embedded dyes also revealed targeting of the particles to damaged, but not undamaged, spinal cord tissues. In an in vivo crush/contusion model of guinea pig SCI, every animal but one injected with PSiNPs recovered conduction through the cord lesion, whereas none of the control animals did. These findings suggest that the use of multifunctional nanoparticles may offer a novel treatment approach for spinal cord injury, traumatic brain injury, and possibly neurodegenerative disorders.

Key words: nanoparticles; nanotechnology; spinal cord injury; membrane sealing; PEG

Spinal cord injury (SCI) is generally considered to be partitioned into two phases: the primary, or mechanical, injury to parenchyma of the cord, followed by a "secondary injury." The latter, which is progressive, can occur over many days and is responsible for the most serious destruction of spinal cord white matter (Borgens and Shi, 2000; Borgens and Bohnert, 2001; Borgens, 2003; Thuret et al., 2006). It is the deterioration of the white matter, comprising axons and not the neurons themselves, that is responsible for the catastrophic behavioral loss after SCI. The primary injury is a mechanical one, producing insult to the membranes of neurons and axons, whereas a cascade of pathological biochemistries largely mediates secondary injury. Furthermore, attacking the problem of secondary injury provides the most opportunity for beneficial intervention in the clinic.

The increase in membrane permeability coincident with a collapse of its "fence" properties permits the unregulated flow of ions into and out of the cell or nerve process. This initiates and accelerates a series of chemical reactions that subsequently leads to cell death or secondary axotomy. This series of catabolic biochemistries is reasonably well understood, beginning with the failure of oxidative metabolism in mitochondria, the formation of highly reactive oxygen species, and their initiation of lipid peroxidation of the inner lamella of the membrane. This latter chemistry leads to the formation of highly toxic endogenous toxins, mainly aldehydes, such as acrolein and hydrononeal (Shi et al., 2002; Luo et al., 2005; Kaminskas et al., 2004; Luo and Shi, 2004, 2005).

Until now, membrane sealing has been accompanied with polymers such as Poloxamer 188 (P188), Poloxamer 1100 (P1100), or polyethylene glycol (PEG). For example, electropermeabilized skeletal muscle membranes were effectively sealed by the action of P188, inhibiting the leakage of an internally sequestered

Contract grant sponsor: General Funds from the CPR (State of Indiana HB 1440); Contract grant sponsor: Mrs. Mari Hulman George.

*Correspondence to: Richard Ben Borgens, PhD, Center for Paralysis Research, School of Veterinary Medicine, Weldon School of Biomedical Engineering, Purdue University, West Lafayette, IN 47907.
E-mail: cpr@purdue.edu

Received 29 May 2009; Revised 6 August 2009; Accepted 8 October 2009

Published online 8 December 2009 in Wiley InterScience (www.interscience.wiley.com). DOI: 10.1002/jnr.22309

fluorescent marker (Lee et al., 1992, 1994; Marks et al., 2001). The amphiphilic properties of P188 facilitate the interaction of lipid bilayers, inducing spontaneous rearrangement of membranes and ultimately reducing the membrane defect. PEG, a well-known membrane fusogen, has also been demonstrated to induce a rapid, nearly immediate recovery of axonal integrity after spinal cord transection in guinea pigs (Shi and Borgens, 1999a; Borgens, 2001). This anatomical fusion and sealing were also associated with a rapid (minutes) recovery of nerve impulse propagation through the original plane of transection (Shi and Borgens, 1999a; Shi and Pryor, 2000b; Borgens et al., 2002). The exact mechanism of action of these polymers in rescuing neuronal integrity, even the fusion of transected axons, is not clear (Nakajima and Ikada, 1994; Lee and Lentz, 1997). However, their safe use and ease of administration in medicine have produced significant recovery of function in adult guinea pig SCI (Davidson and Gerald, 1976; Nakajima and Ikada, 1994; Lee and Lentz, 1997; Working et al., 1997), adult rat brain injury (Koob et al., 2005, 2008), peripheral nerve injury (Donaldson et al., 2002), and clinical cases of canine paraplegia at the University Veterinary Teaching Hospital (Laverty et al., 2004).

In another fast-moving area of medicine, the application of nanotechnology (or nanomedicine) has brought rapid progress in the fields of imaging, diagnostics, and drug and gene delivery (Brannon-Peppas and Blanchette, 2004; Gelperina et al., 2005; Koo et al., 2006; Mohanraj and Chen, 2006; Pathak et al., 2006; Silva, 2007). The key issue in nanomedicine is to deliver constant and concentrated therapeutics to target tissue to minimize their side effects and maximize their efficacy. In this regard, the delivery of therapeutics based on nanoparticle systems is likely to provide considerable benefits over traditional dosing methods: 1) the small size of nanoparticles allows their movement into cells and prevents uptake by phagocytes, 2) the conjugation with drugs/therapeutics provides an ideal and controlled delivery system with specificity and selectivity, and 3) the combination with unique magnetic and luminescence functionalities is useful in various biomedical applications (Zhao et al., 2004; Farokhzad and Langer, 2006; Xu et al., 2007). Recently, we have shown that the application of PEG-coated, silica-based microcolloids (PSMCs) was able to restore structural and physiological function to severely injured mammalian spinal cord by preferentially targeting the damaged tissues (Cho et al., 2008a). In addition, we have reported that the application of hydralazine functionalized mesoporous silica nanoparticle (MSN)-based drug delivery restored damaged cell membranes, allowing improved mitochondria function and abating the effects of the toxin acrolein (Cho et al., 2008b). These results suggest the possibility of PSMCs as a novel therapeutic agent in CNS injury.

These innovations also solve other problems associated with the typical delivery of PEG in sterile saline into the blood stream. The concentration or molecular weight of PEG or P188 has difficulties that limit their beneficial clinical utility. The application of functionalized nanoparticles does not share these limitations and may permit a more significant and beneficial impact in preclinical and clinical study, as will be discussed. The aim of this study was 1) to evaluate membrane sealing ability as well as neuroprotective effects using PEG-functionalized silica nanoparticles (PSiNPs) following spinal cord trauma; 2) to visualize tetramethyl rhodamine-doped PEG-functionalized silica nanoparticles (TMR-PSiNPs) uptake into damaged tissue using photostable, fluorescently labeled particles; and 3) to determine the possible clinical benefits of PSiNPs through animal model testing using somatosensory evoked potentials (SSEP) as an index of physiological recovery in the crushed spinal cord of adult guinea pigs.

MATERIALS AND METHODS

Synthesis and Functionalization of Silica Nanoparticles

All chemicals were purchased from Sigma-Aldrich (St. Louis, MO) unless otherwise specified. Previously we have detailed the fabrication of PEG-coated silica nanoparticles (Cho et al., 2008b). Here we emphasize and extend this to include the attachment of tetramethyl rhodamine (TMR).

TMR-doped silica nanoparticles were synthesized according to the procedure described by Zhao et al. (2004). The mixture, composed of 1.77 ml Triton X-100, 1.8 ml n-hexanol, 7.5 ml cyclohexane, and 0.5 ml of 1% aqueous tetramethyl rhodamine-dextran (TMR-dextran, tetramethylrhodamin 10,000 MW lysine-fixable dextran from Invitrogen, Carlsbad, CA) solution, was prepared to form water-in-oil (W/O) reverse microemulsion. Diluted hydrochloric acid was added to adjust the solution pH to 2.0. After stirring for 30 min, 100 μl of tetraethyl orthosilicate (TEOS) was slowly added to the mixture. The solutions were stirred for another 1 hr and then the polymerization reaction was terminated with the addition of NH_4OH. The determination of particle size is dependent on the concentration of NH_4OH. With higher concentrations of NH_4OH, the larger particles can be produced. The acetone was added to the solution and subsequently collected as a white precipitate by vortexing and centrifugation. Finally, TMR-doped silica nanoparticles were rinsed with ethanol and acetone several times and dried under vacuum at 100°C for 12 hr. The surface modification involved a few steps. First, particles were modified using 3-(trimethoxysilyl) propyl aldehyde (TPA) to obtain aldehyde-terminated functionality. Then, nanoparticles were covalently bonded with PEG by coupling with PEG-NH_2 (M.W. 3000), forming a reactive Schiff's base linkage.

Characterization of TMR-Doped PSiNPs

The size and morphology of TMR-PSiNPs was observed by transmission electron microscope (JEOL 2000FX). To verify the presence of PEG immobilized on the silica surface, Fourier transform-infrared reflection absorption spectroscopy (FT-IRRAS) was employed to evaluate its chemical structure. All data analysis was performed in OMNIC software purchased from the instrument supplier. The resolution of all spectra shown in this paper was 4 cm^{-1}, and in all cases we

collected 100 scans per spectrum. In each synthesis step, data were collected and analyzed from 600 cm^{-1} to 3,600 cm^{-1}. X-ray photoelectron spectroscopy (XPS) was examined to verify the composition of particle using a Kratos Axis Ultra X-ray Photoelectron Spectrometer. Fluorescence intensity of TMR-PSiNPs was measured by Varian eclipse fluorescence spectrometer in a 1-cm quartz cuvette.

Determination of PEG Surface Concentration

The concentration of PEG functionalized onto the silica particle surface was determined by measuring the fluorescent intensity of rhodamine-PEG-NH_2 conjugate (Nanocs Inc.). Silica nanoparticles were modified with rhodamine-PEG-NH_2 through linking with TPA. Varying concentrations of rhodamine-PEG-NH_2 were prepared in DMSO to produce a standard curve. By using a fluorescence spectrometer, the emission intensity of each diluted suspension was measured, and the standard plot was obtained. One milligram ($\sim 1.00 \times 10^{12}$ particles) of silica nanoparticles functionalized with rhodamine-PEG-NH_2 was dispersed into 1 ml ethanol and subsequently diluted to 10^4-fold. The number of rhodamine-PEG-NH_2 molecules coupled to each silica particle was calculated by dividing the rhodamine-PEG-NH_2 reference by the number of particles.

Isolation of Spinal Cord From Guinea Pig and Inducement of Injury

All guinea pigs used in this study were handled in accordance with Purdue Animal Care and Use Committee (PACUC) guidelines. Adult female guinea pigs an average of 623 g were anesthetized with an intramuscular injection of ketamine (60 mg/kg) and xylazine (10 mg/kg). Then, they were perfused through the heart with approximately 500 ml sterile lactated ringer (SLR) solution to remove the blood. The vertebral column was then rapidly removed and a complete dorsal laminectomy performed along the length of the vertebral column, exposing the spinal cord. The spinal cord was carefully removed from vertebrae and immersed in cold, oxygenated Kreb's solution (124 mM NaCl, 2 mM KCl, 1.24 mM KH_2PO_4, 1.3 mM $MgSO_4$, 1.2 mM $CaCl_2$, 10 mM glucose, 26 mM $NaHCO_3$, and 10 mM ascorbic acid). A standardized compression injury was induced with a modified forceps by constant mechanical force for 15 sec. Previously reported investigations of compound action potential (CAP) conduction through whole guinea pig spinal cord using the double sucrose gap isolation/recording chamber (DSGR) verified the immediate and complete loss of conduction through the compression injury produced in this way (Shi and Borgens, 2000; Luo et al., 2002). Compression/contusion injuries are more consistent with clinical injuries and were used in all of the ex vivo and in vivo experiments detailed here but one. Transection of the cord was employed in only the LDH leakage experiments described below. The transection injury was conducted using a miniature scalpel-like cutting tool (No. 10315-12 microscalpel; Fine Science Tools). The segments of spinal cord were immediately immersed in oxygenated Kreb's solution following severe compression or transection of the cord. In all ex vivo and in vivo experiments, the injury site on the spinal cord was approximately midthoracic.

LDH Assay

Membrane integrity associated with injury was also measured by lactate dehydrogenase (LDH) release. LDH, an intracellular enzyme (144 kD), is usually released from cells whose membranes have been injured. In general, 1-cm segments of spinal cord were removed from the midthoracic spinal cord of each animal and incubated in Kreb's solution for at least 1 hr to allow axonal membranes to seal spontaneously from the injury that occurred as a result of tissue isolation (Shi and Pryor, 2000a). This region and procedure were used for all of the biochemical tests described in this report. Segments were then incubated for 10 min in the suspension of uncoated silica nanoparticles, PEG (50% w/w; 2,000 Daltons in DI H_2O), and TMR-PSiNPs (0.1 mg nanoparticles/ml DI H_2O). After rinsing with Kreb's solution three times, samples were incubated for an additional 1 hr in modified Kreb's solution to allow LDH release. LDH leakage was assayed with a TOX-7 kit (Sigma) and normalized for control values from the same animal to control for variation between animals. Five spinal cords from five animals were used for each group.

Targeting Ability of TMR-PSiNPs

TMR-PSiNPs were used to evaluate the distribution of particles and their targeting ability. The segments of spinal cord containing sites of noninjury (intact) and compression injury were incubated in the suspension of TMR-PSiNPs for 15 min, followed by immersion in modified Krebs's solution for another 30 min. The spinal cords were immediately fixed in 4% paraformaldehyde, sectioned with a freezing microtome at 50 μm thickness, and evaluated with a fluorescent microscope using excitation/barrier wavelengths of 545/590 nm, respectively. Labeling with a TMR dye was quantified in NIH Image software by statistically measuring fluorescence (minus background) intensity.

In Vivo Examination of Spinal Cord Conduction Recovery

In total 20 spinal injured adult (350–400 g) guinea pigs were examined into two groups of 10 for in vivo conduction studies. The sham-treated control group received a single subcutaneous injection of lactated Ringers containing uncoated particles, whereas the experimental group received a single subcutaneous injection of PSiNPs solution (0.1 mg PSiNP/ml in sterile injectable Ringers solution), approximately 0.5 hr after SCI.

The midthoracic spinal cord was exposed in deeply anesthetized animals by procedures well described in past papers (Borgens and Bohnert, 2001; Borgens et al., 2002; Silva, 2006), and a constant displacement crushing injury was carried out with a laboratory-fabricated forceps possessing a detente. The wounds were closed in layers, and the animals were allowed to recover under heat lamps to maintain their body temperature. SSEP recordings were carried out on all 20 animals before and after SCI, at 1 day, 1 week, and 2 weeks postinjury. This use of the Nikon-Koden Neuropak

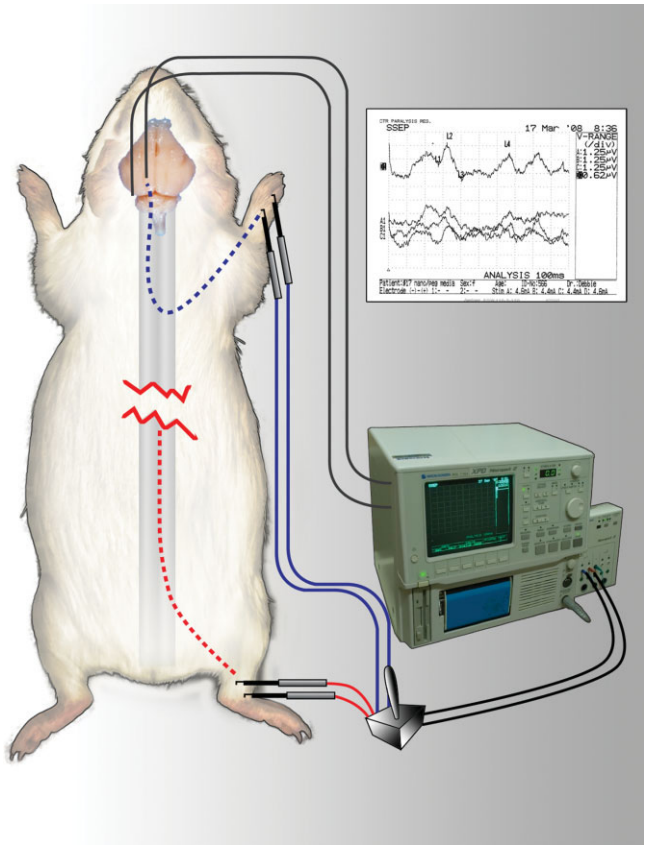

Fig. 1. Recording SSEPs from the adult guinea pig. In the drawing of the animal on the left, the positioning of recording and stimulating electrodes is shown. Pin electrodes were located in the fore and hind limbs to stimulate the medial and tibial nerves, respectively. These electrodes were connected to the stimulator via a toggle that allowed easy switching of stimulation of either neural circuit. Recording electrodes were situated over the contralateral sensorimotor cortex. Prior to any session, this positioning was performed so that a significant SSEP could be recorded from the median nerve circuit, which is unaffected by the midthoracic spinal cord injury. The **inset** is a scan of a complete series of three separate stimulations of the nerve; each record of the three represents 200 repetitive stimulations. These three recordings are shown at the bottom of the record. These are averaged to produce a single averaged SSEP trace, which is shown at the top. Various event markers were used to help determine the character of the recording at later times, as shown here. In all subsequent figures, only the averaged signal is shown.

stimulator/amplifier has been reported in many previous publications (Borgens and Shi, 2000; Borgens et al., 2002); briefly, paired stimulating electrodes were placed under the skin of the foreleg (to excite the medial nerve) and hind leg (to excite the tibial nerve). The investigator could toggle between forelimb and hind limb stimulation by means of a laboratory-fabricated circuit.

Recording electrodes were placed beneath scalp skin on the contralateral side of the body (Fig. 1). Excitation of both limb circuits produced typical evoked potential cascades measured at the contralateral sensorimotor cortex. Typically, the early-arriving potentials were of 40–50 msec latency, with later-arriving peaks measured out to approximately 120 msec. A set of baseline SSEPs was obtained from every animal before SCI. After SCI, SSEPs were still taken in the paired limbs after placement of all electrodes [this time the forelimb (medial nerve/SMC) neural circuit was an effective control for the functioning of the procedure], insofar as this circuit is "above" the level of the lesion and unaffected by it. A "circuit drawing" and a representative record are presented in Figure 1.

Measurement of Superoxide and LPO

Hydroethidine (HE) is one of the reactive oxygen species (ROS) that is responsible for toxic effects in the body via various kinds of tissue damage. It is rapidly converted to ethidium (E^+) in the presence of intracellular superoxide anion (O_2^-) and produces a fluorescent product. Therefore, the level of superoxide can be assessed by the accumulation of ethidium as visualized in specific regions using a fluorescent microscope. The strips of spinal cord were immersed in 1 ml PBS with HE at final concentration of 1 μM for 10 min in the dark. Subsequently, samples were fixed, sectioned, and analyzed with a fluorescent microscope to measure the amount of ethidium bromide uptake. The quantification of lipid peroxidation (LPO) collected from the spinal cord can be an essential clue to demonstrate the deterioration process of the lipids in cell membranes, resulting in cell damage and increased production of free radicals (Gutteridge, 1994; Hall, 1995; Facchinetti et al., 1998; Liu-Snyder et al., 2006a,b). In this study, lipid hydroperoxide assay (Cayman Chemical Company) was used. The compression-injured spinal cords were weighed and homogenized. Once the centrifugation of homogenate at 2,000*g* for 5 min had been performed, lipid peroxides were immediately extracted from the sample into chloroform right before conducting the assay. Upon preparation of the chromogen and sample solution, the absorbance of each sample was read at 500 nm with a spectrophotometer (SLT spectra plate reader). Tissue lipid peroxidation was calculated and expressed as nanomoles per 70 mg wet tissue.

Statistical Analysis

Unless otherwise specified, unpaired Student's *t*-test (for comparison of two groups) or one-way ANOVA and post hoc Newman Keul's test (for more than two groups) was used for statistical analyses (InStat software). Normality was tested by Shapiro-Wilk test (STATA). Equal variances were tested by the method of Barlett for $n \geq 5$ (InStat software) and by less than twofold difference in SD for $n < 5$. Results are expressed as mean ± SD. $P < 0.05$ was considered statistically significant.

RESULTS

Fabrication and Characterization of TMR-PSiNPs

We used 150-nm-diameter PSiNPs for all experiments detailed in this report. We provide further data on the absorption of PEG molecules onto the surface of a range of sizes of dye-doped SiNPs (50, 150, and 300 nm diameters; Fig. 2C). TMR-PSiNPs were synthesized by using multiple procedures. First, hydrophilic

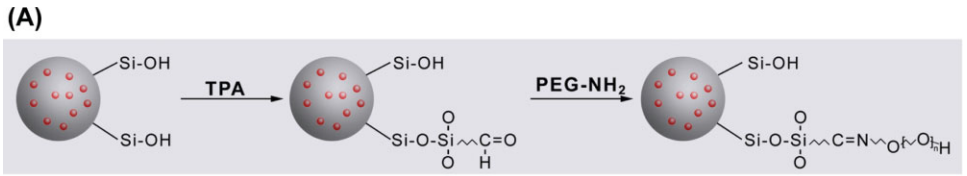

(C)

Particle Size	Avg. amount of chemically coupled PEG (nmol/cm^2)	Avg. amount of chemically coupled PEG (molecules/cm^2)	Avg. amount of chemically coupled PEG (pmol/particle)
50 nm (±8)	2.78 x 10^5	1.67 x 10^{18}	5.6 * 10^{-3}
150 nm (±22)	3.49 x 10^5	2.55 x 10^{18}	7.0 * 10^{-3}
300 nm (±39)	3.79 x 10^5	2.71 x 10^{18}	7.6 * 10^{-3}

Fig. 2. Schematic synthesis and characterization of TMR-doped PEG-functionalized silica nanoparticles (TMR-PSiNPs). **A:** Organic dye-doped silica nanoparticles were synthesized by water-in-oil (W/O) microemulsion, in which tetramethyl rhodamine (TMR) dextran was added to the microemulsion solution. The silica polymerization reaction is begun by the addition of tetramethyl orthosilicate (TEOS) and terminated by the addition of NH_4OH. Covalent immobilization of PEG was performed by conjugation with 3-(trimethoxysilyl) propyl aldehyde (TPA) and subsequent coupling with PEG-NH_2 (MW 3,000) onto the silica surface. The particles were separated from the microemulsion by vortexing and centrifugation in acetone and ethanol, respectively. **B:** TEM image of TMR-PSiNPs with a diameter of 150 nm. The **inset** is a significant magnification to show the TMR dextran as a black inclusion within the silica network. **C:** Summary table of the concentrations of PEG molecules immobilized on silica surfaces of different sizes. Rhodamine-PEG-NH_2 solutions of different concentrations were prepared and measured to obtain standard curves. The number of rhodamine-PEG-NH_2 molecules coupled to each silica particle was determined by fluorescence spectrometer using linear equations. We used the 150-nm-diameter TMR-PSiNPs for all experiments reported here. [Color figure can be viewed in the online issue, which is available at www.interscience.wiley.com.]

organic dye molecules, TMR-dextran, were entrapped into the silica pores during polymerization of TEOS by strong electrostatic interaction that was achieved by adding an acidic solution during a reverse microemulsion process. Then, the silica surface was functionalized with aldehyde groups by treatment with TPA. Consequently, PEG-NH_2 was attached to the aldehyde moiety through Schiff's base linkage. Figure 2A illustrates the synthesis of organic dye-incorporated silica particles and further covalent conjugation with PEG. Figure 2B shows typical TEM images of nanoparticles with mean diameter of 150 nm. The higher magnification image details the presence of TMR-dextran as black dots (Fig. 2, inset). The silica network serves as a shield or barrier to prevent the dye (TMR) from escaping, retaining its luminophore activity. We also determined the surface coverage of PEG derivatives linked to silica particles of different sizes, ranging between ~50 and 300 nm, by using a fluorescence-based method (illustrated in Fig. 2C). Fluorescent spectroscopy calculated the concentration of PEG-rhodamine molecules after removal of the silica matrix by treatment with hydrofluoric (HF) acid solution. The silica nanoparticles coated with PEG-rhodamine molecules were immersed in aqueous HF overnight in the dark to remove the silica matrix. The interpolation of fluorescent intensity measured at 590 nm with a standard linear calibration curve was capable of determining the concentration of PEG molecules. Five free PEG-rhodamine molecules with different known concentrations were prepared to construct standard curves. As a consequence, the average amount of PEG molecules per particle was obtained by dividing the measured PEG concentration by the original silica nanoparticle concentration.

As previously reported (Cho et al., 2008a), we established the chemical composition of surface properties by Fourier transform infrared (FT-IR) spectrometer and X-ray photoelectron spectroscopy (XPS) after PEG modification of the silica surface. The characteristic peaks of C-H bonding at ~2,800–3,000 and ~1,400–1,500 cm^{-1} were indicative of the presence of PEG molecules on the silica surface. In addition, the appearance of C 1s and N 1s peak in XPS spectra confirms the chemical structure of the molecular species present on the silica surface (refer to Cho et al., 2008a). The advantage of incorporation of organic dye inside the silica matrix is the enhancement of photostability, preventing photobleaching even after multiple uses. Furthermore, this ''caging effect'' generated from entrapment of the fluorescent dye contributes to the significant increase of fluorescent intensity. Figure 3 shows the excitation and emission spectra between free TMR dye (Fig. 3C,D) and TMR-PSiNPs (Fig. 3A,B). Although the molar concentration of TMR-PSiNP (1×10^{-9} M) is lower by four orders of magnitude compared with free TMR (1×10^{-5} M), the fluorescent signal of the former is considerably higher in both photoexcitation and photoemission. To assess whether the silica coating was advantageous, i.e., remaining photosensitive, we

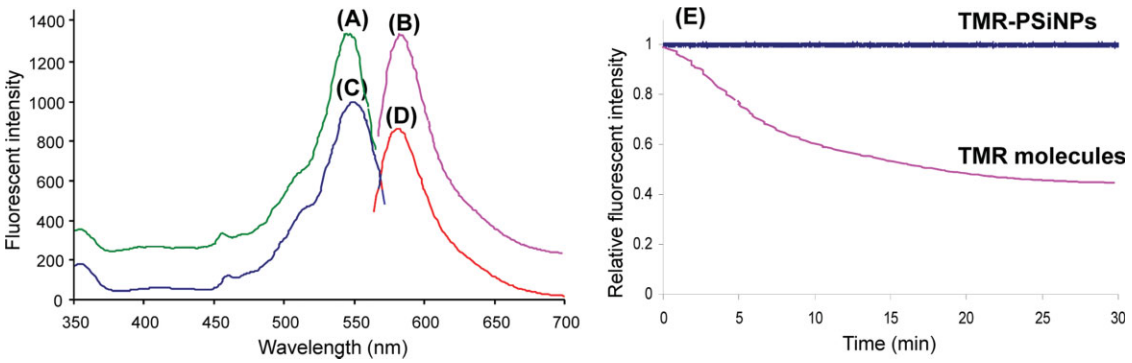

Fig. 3. Fluorescent excitation and emission spectra of TMR-PSiNP. Fluorescent excitation and emission spectra of TMR-PSiNP (**A,B:**) and free TMR (**C,D**) molecules in water. Although the concentration of TMR-PSiNP (1×10^{-9} M) is lower than that of free TMR (1×10^{-5} M), the fluorescent intensity is higher in both photoexcitation and photoemission by four orders of magnitude. **E:** Comparison of fluorescent intensity of TMR-PSiNP vs. TMR molecules in water as a function of time to evaluate this photostability further. By continuous excitation with an Xe lamp, fluorescent intensity of free TMR molecules was significantly reduced, whereas that of TMR-PSiNP shows almost no photobleaching. [Color figure can be viewed in the online issue, which is available at www.interscience.wiley.com.]

conducted photobleaching tests using the aqueous phase of TMR dye and TMR-PSiNPs. Figure 3E shows that substantial photobleaching in TMR-PSiNPs did not occur even after continuous exposure to fluorescent excitation for 30 min. This result was compared with that of TMR dye alone, which showed a gradual decrease in fluorescent intensity with excitation time.

Ex Vivo Application of TMR-PSiNPs to Injured Mammalian Spinal Cord

Our main purpose in fabricating and characterizing PSiNP was to evaluate the therapeutic value after attachment to damaged CNS tissue and cells. We quantified the resealing of damaged membranes by measuring the leakage of the enzyme LDH (144 kD) into the extracellular milieu. When the cell membrane is injured, significant leakage of LDH occurs, which can be assayed in the extracellular fluid. Transection of the cord was used only in this experiment because it produces the maximal amount of LDH leakage possible. This makes it possible to determine even ''low'' levels of sealing produced by the experimental intervention compared with controls.

In Figure 4, LDH concentration was significantly increased in the supernatant over background leakage by transection of the tissue. Treatment with PSiNPs or PEG alone significantly reduced the level of LDH loss to control levels ($P = 0.005$; Fig. 4). In addition, the ''control'' application using bare silica nanoparticles (SiNP) did not seal the tissues; LDH leakage was similar to that measured after injury. Figure 5 shows the correlation of the PEG concentration of PSiNPs vs. PEG alone. The LDH release after treatment with PEG alone or PSiNP was significantly reduced compared with controls ($P = 0.05$, and $P = 0.001$, respectively; Fig. 5). However, the effective concentration of PEG was lower by two orders of magnitude when delivered by nanoparticles (Fig. 5). As the concentration of PEG on particles increased from 2.5×10^{-4} M to 1.3×10^{-3} M, the

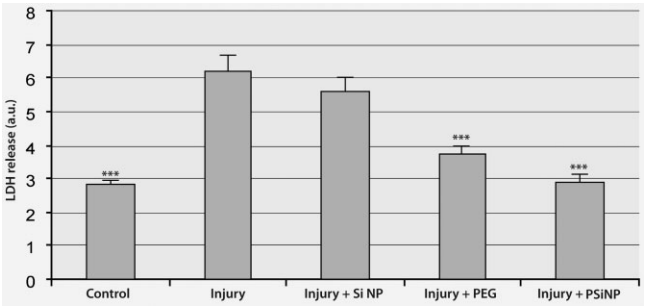

Fig. 4. Evaluation of membrane sealing using lactate dehydrogenase (LDH). The leakage of LDH (144 kD) enzyme from the cytosol to the extracellular medium is an indicator of membrane integrity. The spinal cords in each group (e.g., control, injured, injured and PEG-treated, injured and Si nanoparticle-treated, and injured and PSiNP-treated spinal cords) were incubated in Krebs solution for about 3 hr. The supernatant was collected, and the LDH concentration was determined. Transection injury to the cord significantly enhanced the leakage of LDH into the supernatant compared with its typical background loss, whereas treatment with PEG-coated particles reduced the level of LDH to control levels. The results are expressed as percentage control values ± SD (n = 5). One-way paired ANOVA and post hoc Newman Keul's test were used for statistical analysis. ***$P < 0.005$.

level of LDH leakage was linearly decreased from 52% ± 7.8% to 26% ± 3.5% of control values. PEG-treated cords also displayed a similar trend in concentration-dependent effects on LDH release.

Targeting Ability of TMR-PSiNP Following Traumatic SCI

To examine and compare PEG distribution in injured and uninjured spinal cord tissues, TMR-PSiNP was applied after a standardized compression injury (Fig. 6). Crushed cords were incubated in the TMR-PSiNP solution for 15 min, followed by immersion in

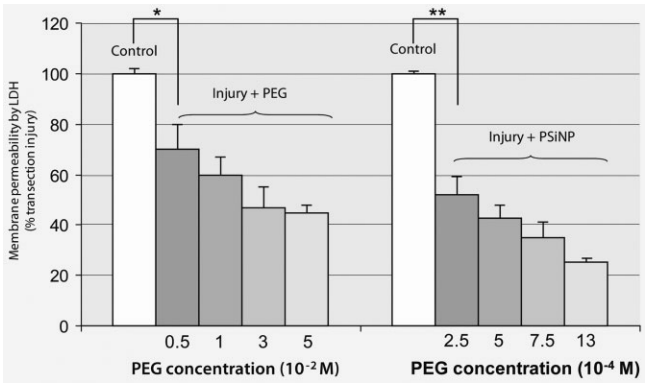

Fig. 5. Membrane permeability: PEG and PSiNPs. The result of the membrane permeability evaluation is shown as a function of the concentration of PEG-functionalized silica nanoparticles and PEG molecules alone. Completely transected spinal cords were exposed to PEG-functionalized silica nanoparticles or a PEG solution for 15 min. Subsequently, spinal cords in each treatment group were immersed in Krebs solution for about 3 hr, the supernatant was collected, and LDH concentrations were determined. The reduction in membrane permeability in response to PEG-functionalized silica particles was similar to that of PEG-treated spinal cords, even though the concentration of PEG was reduced by two orders of magnitude when delivered by nanoparticles. Results are expressed as a percentage of the uninjured values ± SD (n = 5). $\star P < 0.05$, $\star\star P < 0.001$.

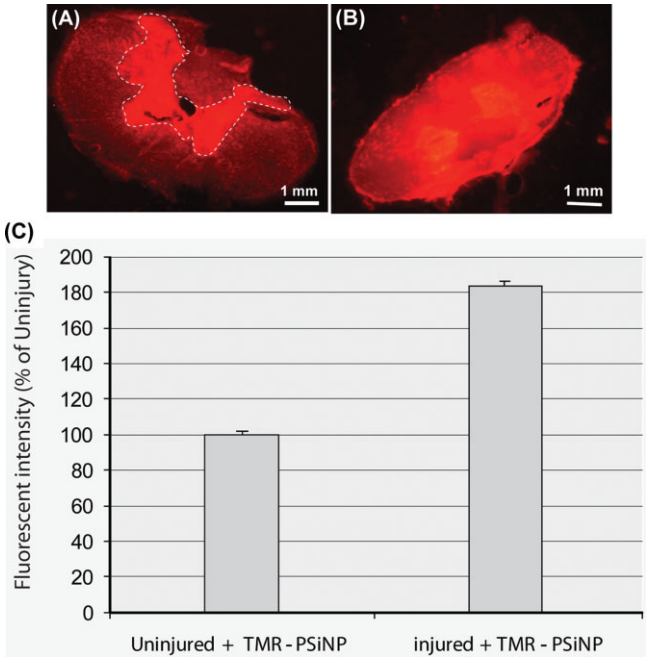

Fig. 6. Targeting of injured parenchyma by TMR-PSiNPs. Selective discrimination of injured vs. uninjured spinal cord tissue in crushed spinal cord is shown by fluorescence microscopy. After standardized compression of the spinal cord (see Materials and Methods), TMR-PSiNP was applied to the area of injury for 15 min and the spinal cord subsequently immersed in Krebs' solution for 30 min. Fluorescence microscopy of 50-μm-thick frozen sections was used to reveal labeling in both injured and uninjured cords. **A:** Typical control (uninjured) cord section obtained from segment of spinal cord approximately four vertebral segments distant from the injury site shows a faintly labeled white matter, especially heavier in gray matter (hatched line). **B:** Similar sample of crushed spinal cord section with the histological section obtained from the approximate center of the region of compression shows significant labeling by particles. **C:** Quantitation of fluorescent intensity in injured and uninjured spinal cord with background fluorescence normalized and with the subtraction of background fluorescence (see Materials and Methods). Results are expressed as a percentage of the uninjured values ± SD (n = 3).

oxygenated Krebs for an additional 30 min. The crushed regions of the cord were intensely labeled in both gray and white matter. The white matter of the uninjured segments of cord was labeled poorly, sometimes undetectably (100% ± 2%), whereas gray matter was more detectable. In the injured region of the spinal cord, the accumulation of TMR-PSiNPs at the lesion, including both gray and white matter, was marked (182% ± 3%). The gray matter of uninjured cord was still labeled, although sealing significantly reduced fluorescent intensity considerably lower than that of gray matter in damaged spinal cord.

PSiNPs Block the Generation of Membrane Lipid Peroxidation and Superoxide Following SCI

To assess whether the exposure of PSiNPs to damaged spinal cord tissues could significantly attenuate the rate of ROS and LPO production, we analyzed ROS-mediated oxidative stress propagation, LPO generation, and their reduction. Fluorescent oxidation assays were used to detect ROS production. As shown in Figure 7, superoxide generation was elevated in the lesioned spinal cord, and the application of PSiNP significantly reduced this up-regulation from 202% ± 32% to 100% ± 22% of that in the control group. This indicates a more than 100% decrease in the injury-associated enhancement of ROS. In the injured-SiNP group, reduction of ROSs did not occur (190% ± 38% of control group). In contrast, the injured-PEG group resulted in a decrease in ROS production (165% ± 30% of control group) compared with the injury group. We then monitored the effect of PSiNP on LPO following compression injury, in which LPO was measured by a standard tissue assay (Fig. 8). The reduction of LPO was similar to the measured ROS reduction. LPO levels in the injury group were 51 ± 4 nmol/70 mg compared with the control group (22 ± 4.5 nmol/70 mg). The application of PEG and PSiNP significantly attenuated the level of LPO to 33 ± 2 nmol/70 mg and 31 ± 2 nmol/70 mg, respectively. As expected, the addition of uncoated SiNP to the medium did not show any significant change (45 ± 0.5 nmol/70 mg) compared with the injury group.

Recovery of Conduction in the Injured Spinal Cord

Injection of PSiNPs led to a statistically significant recovery of SSEP conduction through the lesion in the treated group. Fourteen of the fifteen PEG-coated-

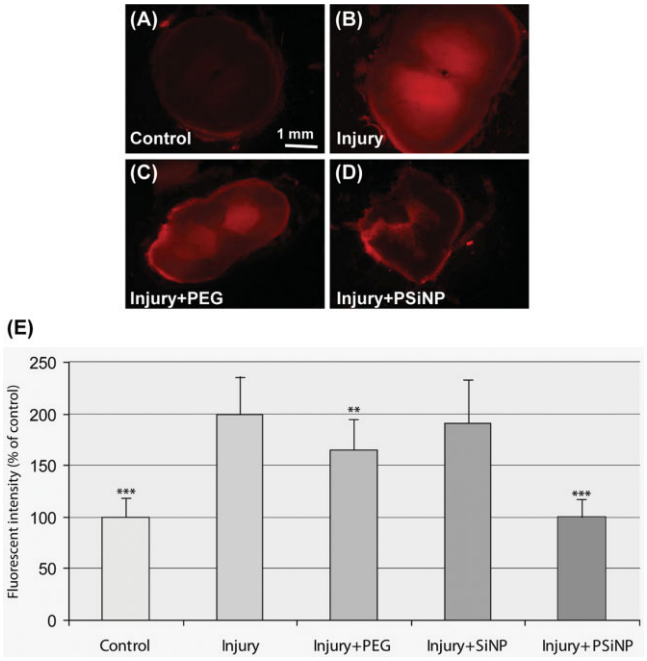

Fig. 7. Evaluating function in the spinal cord of the adult guinea pig. The effects of spinal cord compression injury and TMR-PSiNP treatment on the magnitude of ROS generation. **A–D** are representative fluorescent micrographs showing the intensity of oxidized hydroethidine (HE) in the control-uninjured spinal cord (A), injured but untreated spinal cord (B), injured but PEG-treated spinal cord (C), and injured and PSiNP-treated spinal cord group (D). The treatment with PSiNP and PEG was followed immediately after standardized cord compression. The compression injury increased the level of oxidized HE, whereas PSiNP posttreatment inhibited it. The enhancement of this effect by PSiNPs was apparent even by qualitative viewing of these histological sections (compare C and D). **E:** Quantification of oxidized HE fluorescence intensity (n = 5, $\star\star P < 0.001$, $\star\star\star P < 0.005$). Note that PSiNP treatment significantly reduces the production of oxidized HE compared with PEG.

particle–injected animals recovered the SSEP, as stimulated from the tibial nerve; seven within 3 days of the injury, two more within 9 days of the injection, and five more by 2 weeks after treatment. None of the controls showed any recovery of the SSEP by the 9-day time point ($P = 0.02$; Fisher's exact test; Fig. 9). By 2 weeks, all but one PSiNP treated animals had recovered the SSEP compared with a lack of clear conduction of the SSEP in animals that received uncoated particles ($P = 0.0005$; Fisher's exact test). One of these control animal's physiological recordings was unstable (''noisy''), so, even if we conservatively scored this record as indicating recovery, still the statistical improvement in recovery of evoked potential conduction in response to PSiNP was impressive ($P = 0.006$; Fisher's exact test; Fig. 10). Overall, a ''control'' stimulation of the medial nerve circuit was positive, revealing that, had EP conduction passed the lesion, it would have been recorded at the contralateral sensorimotor cortex.

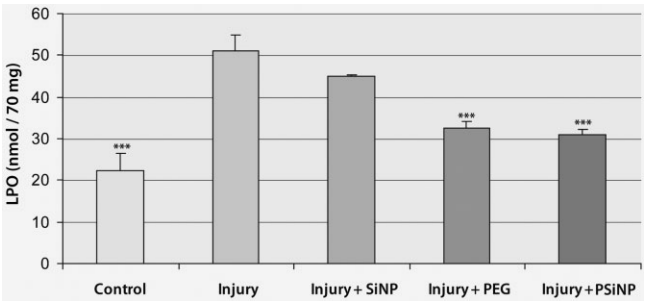

Fig. 8. LPO reduction by PSiNP. The level of LPO after compression injury and subsequent application of PSiNP indicated that compression injury induces significant elevation in the level of LPO, whereas PSiNP exposed spinal cords significantly reduced it (n = 5, $\star\star\star P < 0.005$).

DISCUSSION

Overview

1) We have both described and characterized PSiNPs coated with the fusogen PEG. 2) By incorporating a fluorescent label (TMR) to the PSiNPs, we have shown that these particles preferentially target injured spinal cord parenchyma, particularly white matter. The labeling of injured white matter in compression-injured control spinal cords was nearly nullified by treatment with PSiNPs. 3) Application of PSiNPs in ex vivo preparations sealed compromised cells after crush injury to the cord. The enhanced leakage of the large enzyme LDH from the cytoplasmic compartment of cells was suppressed to control values by the addition of PSiNPs. Furthermore, indicators of secondary injury processes resulting from mechanical injury such as ROS up-regulation and LPO of membranes were both significantly reduced by PSiNPs. 4) Moreover, PSiNPs can restore function in a guinea pig SCI model. Sealing of axolemmas by PSiNPs, but not SiNPs, was thus complete enough to restore physiological functioning to white matter. The recovery of evoked potentials traversing the spinal cord lesion—stimulated in the hind limb of adult guinea pigs and recorded at the sensorimotor cortex of the brain—was restored by injection of PsiNPs, but not SiNBPs. This phenomenon was first observed and recorded in double sucrose gap recording and isolation chamber in real time (Cho et al., 2008a). This unique isolation/recording chamber allows highly sensitive, real-time measurement of CAPs traversing full-length samples of guinea pig or rat spinal cords (Shi and Borgens, 1999a,b, 2000; Luo et al., 2002). This observation was duplicated and extended here in adult guinea pigs by SSEP techniques.

The application of nanoparticles in the biomedical field has had considerable impact in the improvement of diagnosis thorough sensitive imaging, particularly at the early stage of disease, and enhancement of effective therapeutics (Duncan, 2003; Emerich and Thanos, 2006; Wang et al., 2006). Fluorescent dyes incorporated within

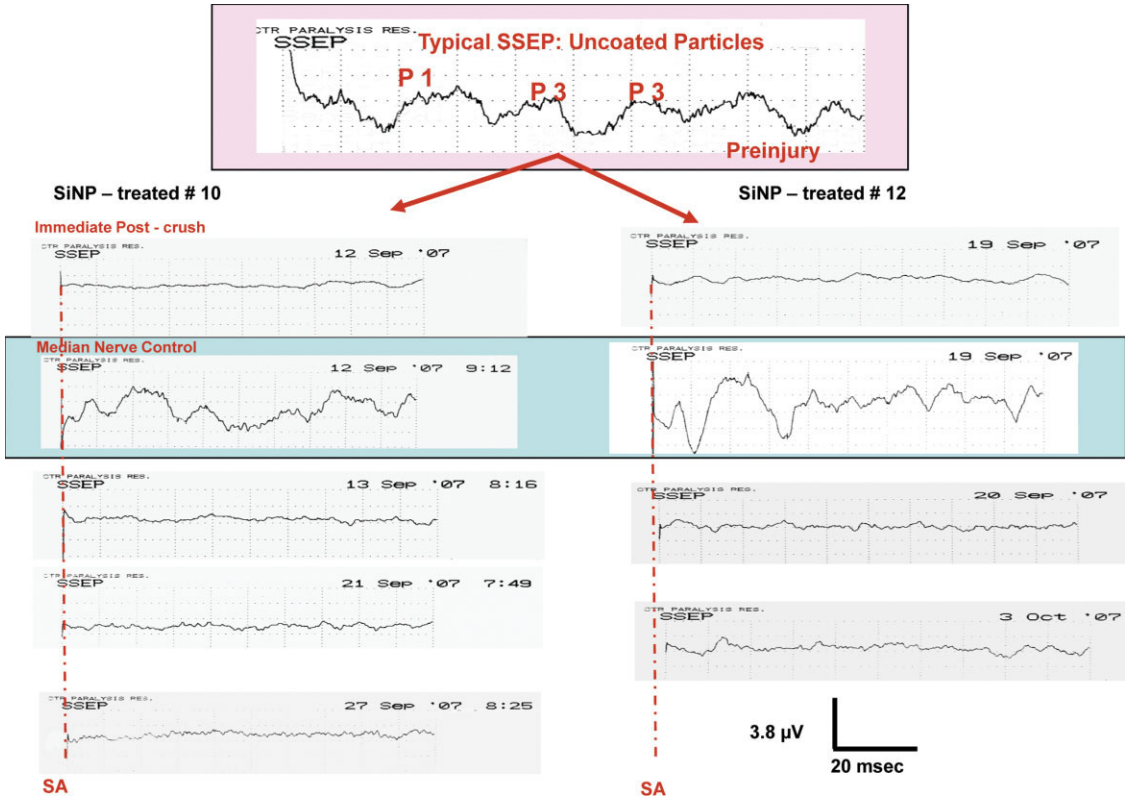

Fig. 9. Failure to recover conduction with uncoated nanoparticles. Top panel shows an SSEP electrical record obtained from a control animal that received a subcutaneous injection of uncoated particles (SiNP; 0.1 mg particles/ml sterile injectable Ringers solution). Note the characteristic three peaks in the evoked potential: the earliest about 30 msec after stimulation and two others approximately 15–20 msec apart. Later-arriving potentials were often recorded, as shown here, but were more variable in appearance and in their latency. The first and second columns are records taken from control animals 10 and 12, respectively. Note the complete collapse of evoked potentials immediately (within 20 min) after the crush injury to the spinal cord. Records taken at this same time from the medial nerve circuit revealed that strong SSEPs could be recorded at the cortex. Note the continued failure to respond to tibial nerve stimulation in the days and weeks subsequently. Such records were typical of every control animal in the series. [Color figure can be viewed in the online issue, which is available at www.interscience.wiley.com.]

silica particles provide several attractive features for probing molecular and cellular processes (Santra et al., 2001; Liu et al., 2007; Yan et al., 2007). Unlike conventional organic fluorescent dyes, the fluorescent probes embedded within nanoparticles are more photostable, bright, and effective as markers. This capacity has enhanced our ability to determine that PSiNPs preferentially target injured white matter. These results compare favorably with the injection of PEG (~30% in lactated Ringers) to both compression-injured spinal cords in guinea pigs and after traumatic brain injury in rats (Shi et al., 2002; Koob et al., 2005). The concentration of PEG attached to 1 mg of silica particles (5.6 mmol/ml) is relatively low compared with that of PEG alone in injectable Ringers (50 mmol/ml). However, the therapeutic value to disrupted membranes in the former is immeasurably greater, because of the high concentration of the polymer attached to each particle, in concert with the actually immeasurable concentration of particles themselves that attach to the injury site.

In summary, the interaction of PSiNPs with damaged axonal membranes facilitates spontaneous reorganization of the compromised membrane, rapidly promotes anatomical sealing, and permits the near-immediate recovery of conduction through guinea pig spinal cord white matter. We have emphasized a particle diameter of ~150 nm. Usually, the cellular internalization is governed by the particle diameter used. Once particles are administered into the body, particles with diameters larger than 400 nm are primarily cleared via phagocytosis by macrophages, whereas small particles less than 50 nm cause serious interparticle aggregation and exhibit less effective capabilities. Consequently, particles in the range of ~100–200 nm seem to be the best in biological usage. Furthermore, the use of particles facilitates the internalization of PEG molecules into the cytoplasm of the injured cell through endocytosis (Cho et al., 2008b).

Restoration of Disrupted Plasma Membrane by the Application of PEG

Traumatic SCIs lead to many and varied complications with respect to movement and sensation in the body. This pathology accompanies the destruction of

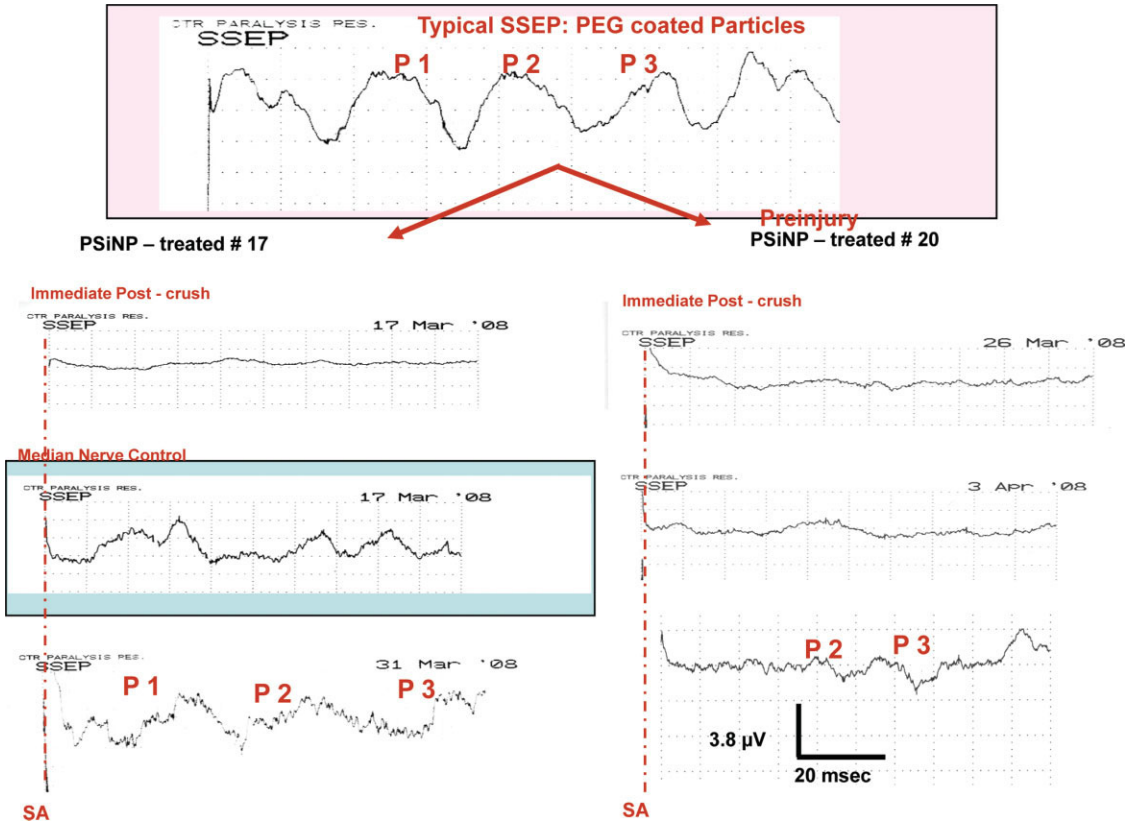

Fig. 10. Recovery of SSEP conduction using PSiNPs. The **inset** shows an electrical recording obtained from an experimental animal that was typical of every animal in the treated series prior to the compression of the spinal cord and the collapse of that evoked potential immediately after injury. Rows 1 and 2 are electrical records taken from experimental animals 17 and 20, respectively. Note that for animal 17 a medial nerve control recording is provided, showing that, if the cord were competent to respond to stimulation, an SSEP would have been observed at the cortex. This animal is typical of the best responders in the series injected subcutaneously with 0.1 mg PSiNP/ml sterile injectable Ringers solution. Animal 20 was the worst responder of the series. After 2 weeks duration, the evoked potentials recorded from tibial nerve stimulation were weak, with an uncharacteristic longer latency. We surmise based on the delay that P1 had not yet recovered. [Color figure can be viewed in the online issue, which is available at www.interscience.wiley.com.]

largely white matter by progressive secondary injury that begins immediately after the initial mechanical, or ''primary,'' injury. This delayed biochemically mediated injury in association with ischemia and other vascular issues initiates the more profound progressive cell and tissue destruction processes and ultimately permanent behavioral loss. The most recent clinical efforts have been aimed at reducing the extent of damage by effective drug therapy rapidly after injury such as tested in the NASCIS trials of the 1980s and 1990s. Based largely on the notion of interference with antioxidant-mediated destruction of cells during the secondary injury process, these attempts have failed to produce an effective therapy (Coleman et al., 2000).

Although the attempt to interfere with ''free radicals'' has a long and laudable history in SCI, recent investigation suggests that this is not the most effective way to interrupt the free radical/lipid peroxidation cascade ultimately leading to cell death after CNS damage. Highly reactive oxygen species are products of the collapse of mitochondrial function and their oxidative metabolism, accelerating the overproduction of the oxygen radicals themselves via positive feedback. However, catabolism of the inner lamella of the membrane leading to climbing aldehyde production, such as that of acrolein and the associated constellation of related aldehyde cellular toxins (Luo et al., 2004), is the more significant problem. Our previous data indicate that PEG is capable of ''sealing'' membrane disruption, reducing the exchange of ions through the cellular lesion, which then reduces initial ROS and LPO generation (Shi et al., 2002; Luo et al., 2005; Luo and Shi, 2004, 2005; Liu-Snyder et al., 2007). Insofar as LPO is facilitated by the biochemical processes, it is no surprise that the occurrence of LPO is reduced by the action of the PEG surface coat on PSiNPs but is not completely eliminated. Although PEG appears to act like an antioxidant by reducing ROS, it is not a free radical scavenger (Luo et al., 2002). Its beneficial activity is expressed by specific targeting of damaged neurons and white matter after SCI and TBI (Shi et al., 2002) and the capability to seal the plasma membrane immediately, leading to

spontaneous reassembly of the defective membrane (Borgens, 2001). The exact molecular mechanisms underlying PEG's (and other ''sealants'') effect of closure and spontaneous reassembly of the compromised portion of the cell membrane are still an active area of investigation (Lee et al., 1992; Borgens, 2003). This ability is believed to reside in the hyper-/hydrophilicity of the polymers that alter the organization of water at and/or near the region of damage, permitting the hydrophobic core to resolve together in an unbroken lamina (see Borgens, 2003). Interference with the destructive biochemical cascades produced by collapse of the ''fence'' properties of the membrane is then reduced significantly through the restructuring of the membrane itself.

The polymer-related reduction of the biochemically based driving force for the local destruction of white matter provides significant behavioral recovery after SCI (Borgens, 2001; Borgens and Bohnert, 2001; Borgens et al., 2004) and traumatic brain injury (Koob et al., 2005, 2008). Indeed, clinical trials using naturally injured paraplegic dogs revealed significantly enhanced recovery from SCI (Laverty et al., 2004).

A clinical SCI is usually of less than one vertebral segment in extent, so the loss of gray matter (neurons) plays little role in the catastrophic behavioral loss in SCI. The latter is due acutely to the separation of white matter (composed of only axons) completely inhibiting transmission of evoked potentials between the two ''segments'' of the body. Thus the singular and significant targeting of damaged white matter by PEG and PSiNPs is the key to behavioral recovery in SCI. However, in traumatic brain injury, bioavailability issues are much more critical. We have previously reported this in detail (see Koob et al., 2005, 2008).

PSiNP vs. PEG in Suspension

The nanoparticle-based PEG delivery system provides considerable potential over free PEG in suspension. First, a more effective sealing by PEG alone that would be clinically practicable is limited by concentration and the choices of molecular weight. Higher concentrations of PEG in sterile saline greater than 30% W/W lead to more viscous solutions that are not as useful for administration to the blood supply. Reducing viscosity by the choice of lower molecular weights (<1,000 Daltons) could be dangerous, insofar as the monomer (ethylene glycol) is highly toxic (Brent, 2001; Caravati et al., 2005) and its concentration in the blood would be climbing by breakdown of PEG dimers and trimers. Such concentration-dependent effects are nullified by application of the PEG colloids and silica nanoparticles, which themselves are nontoxic (Zhao et al., 2004). Second, a nanoparticle-PEG conjugate system improves PEG bioavailability through enhanced cellular uptake capability and allows the direct interaction with cell compartments, especially possibly disrupted mitochondria membrane. Nanoparticles coated with PEG have been observed to be imbibed through the repaired membrane by endocytosis as can be seen in Figure 4 of Cho et al. (2008b). According to another previous report (Luo et al., 2002), the bulkiness of PEG molecules inhibits such cellular internalization when deposited on the surface of cell. The limitation has been further shown to inhibit a robust effect on inhibiting acrolein-mediated cell damage in vitro, and significant delay in PEG application after traumatic brain injury (>4 hr; Koob et al., 2005) is also associated with a loss in its therapeutic value in ameliorating behavioral loss after traumatic brain injury (Koob et al., 2008). In vivo testing has indicated the biodistribution of silica particles in the body, ion which silica nanoparticles were trapped in the spleen and liver and were lost gradually through normal excretion (i.e., urine; Barbé et al., 2004). The application of PEG-decorated silica nanoparticles provides a larger therapeutic window via 1) lower overall drug level relative to PEG dissolved in the blood and 2) specific targeting of the lesion, coincident with extraordinary high, perhaps immeasurably high, concentrations of the effective agent on compromised cell surfaces.

ACKNOWLEDGMENT

We thank Debra Bohnert for her expert handling of whole-animal experiments.

REFERENCES

Barbé C, Bartlett J, Kong L, Finnie K, Lin HQ, Larkin M, Calleja S, Bush A, Calleja G. 2004. Silica particles: a novel drug-delivery system. Adv Materials 16:1959–1966.

Borgens RB. 2001. Cellular engineering: molecular repair of membranes to rescue cells of the damaged nervous system. Neurosurgery 49:370–378; discussion 378–379.

Borgens RB. 2003. Restoring function to the injured human spinal cord [monograph]. Heidelberg: Springer-Verlag. III–IV, 1–155 p.

Borgens RB, Bohnert D. 2001. Rapid recovery from spinal cord injury following subcutaneously administered polyethylene glycol. J Neurosci Res 66:1179–1186.

Borgens RB, Shi R. 2000. Immediate recovery from spinal cord injury through molecular repair of nerve membranes with polyethylene glycol. FASEB J 14:27–35.

Borgens RB, Shi R, Bohnert D. 2002. Behavioral recovery from spinal cord injury following delayed application of polyethylene glycol. J Exp Biol 205:1–12.

Borgens RB, Bohnert D, Duerstock B, Spomar D, Lee RC. 2004. Subcutaneous tri-block copolymer produces recovery from spinal cord injury. J Neurosci Res 76:141–154.

Brannon-Peppas L, Blanchette JO. 2004. Nanoparticle and targeted systems for cancer therapy. Adv Drug Deliv Rev 56:1649–1659.

Brent J. 2001. Current management of ethylene glycol poisoning. Drugs 61:979–988.

Caravati EM, Erdman AR, Christianson G, Manoguerra AS, Booze LL, Woolf AD, Olson KR, Chyka PA, Scharman EJ, Wax PM, Keyes DC, Troutman WG. 2005. Ethylene glycol exposure: an evidence-based consensus guideline for out-of-hospital management. Clin Toxicol 43:327–345.

Cho Y, Shi R, Borgens R, Ivanisevic A. 2008a. Repairing the damaged spinal cord and brain with nanomedicine. Small (in press).

Cho Y, Shi R, Borgens RB, Ivanisevic A. 2008b. Functionalized mesoporous silica nanoparticle-based drug delivery system to rescue acrolein-mediated cell death. Nanomedicine 3:507–519.

Coleman WP, Benzel D, Cahill DW, Ducker T, Geisler F, Green B, Gropper MR, Goffin J, Madsen PW 3rd, Maiman DJ, Ondra SL, Rosner M, Sasso RC, Trost GR, Zeidman S. 2000. A critical appraisal of the reporting of the National Acute Spinal Cord Injury Studies (II and III) of methylprednisolone in acute spinal cord injury. J Spinal Disord 13:185–199.

Davidson RL, Gerald PS. 1976. Improved techniques for the induction of mammalian cell hybridization by polyethylene glycol. Somat Cell Genet 2:165–176.

Donaldson J, Shi R, Borgens R. 2002. Polyethylene glycol rapidly restores physiological functions in damaged sciatic nerves of guinea pigs. Neurosurgery 50:147–156.

Duncan R. 2003. The dawning era of polymer therapeutics. Nat Rev Drug Discov 2:347–360.

Emerich DF, Thanos CG. 2006. The pinpoint promise of nanoparticle-based drug delivery and molecular diagnosis. Biomol Eng 23:171–184.

Facchinetti F, Dawson VL, Dawson TM. 1998. Free radicals as mediators of neuronal injury. Cell Mol Neurobiol 18:667–682.

Farokhzad OC, Langer R. 2006. Nanomedicine: developing smarter therapeutic and diagnostic modalities. Adv Drug Deliv Rev 58:1456–1459.

Gelperina S, Kisich K, Iseman MD, Heifets L. 2005. The potential advantages of nanoparticle drug delivery systems in chemotherapy of tuberculosis. Am J Respir Crit Care Med 172:1487–1490.

Gutteridge JM. 1994. Hydroxyl radicals, iron, oxidative stress, and neurodegeneration. Ann N Y Acad Sci 738:201–213.

Hall ED. 1995. Inhibition of lipid peroxidation in central nervous system trauma and ischemia. J Neurol Sci 134(Suppl):79–83.

Kaminskas LM, Pyke SM, Burcham PC. 2004. Reactivity of hydrazinophthalazine drugs with the lipid peroxidation products acrolein and crotonaldehyde. Organ Biomol Chem 2:2578–2584.

Koo YE, Reddy GR, Bhojani M, Schneider R, Philbert MA, Rehemtulla A, Ross BD, Kopelman R. 2006. Brain cancer diagnosis and therapy with nanoplatforms. Adv Drug Deliv Rev 58:1556–1577.

Koob AO, Duerstock BS, Babbs CF, Sun Y, Borgens RB. 2005. Intravenous polyethylene glycol inhibits the loss of cerebral cells after brain injury. J Neurotrauma 22:1092–1111.

Koob AO, Colby JM, Borgens RB. 2008. Behavioral recovery from traumatic brain injury after membrane reconstruction using polyethylene glycol. J Biol Eng 2:9.

Laverty PH, Leskovar A, Breur GJ, Coates JR, Bergman RL, Widmer WR, Toombs JP, Shapiro S, Borgens RB. 2004. A preliminary study of intravenous surfactants in paraplegic dogs: polymer therapy in canine clinical SCI. J Neurotrauma 21:1767–1777.

Lee J, Lentz BR. 1997. Evolution of lipidic structures during model membrane fusion and the relation of this process to cell membrane fusion. Biochemistry 36:6251–6259.

Lee RC, River LP, Pan F-S, Wollman RS. 1992. Surfactant-induced sealing of electrpermeabilized skeletal muscle membranes in vitro. Proc Natl Acad Sci U S A 89:4524–4528.

Lee RC, Myerov A, Maloney CP. 1994. Promising therapy for cell membrane damage. Ann N Y Acad Sci 720:239–245.

Liu-Snyder P, Borgens RB, Shi R. 2006a. Hydralazine rescues PC12 cells from acrolein-mediated death. J Neurosci Res 84:219–227.

Liu-Snyder P, McNally H, Shi R, Borgens RB. 2006b. Acrolein-mediated mechanisms of neuronal death. J Neurosci Res 84:209–218.

Liu-Snyder P, Logan MP, Shi R, Smith DT, Borgens RB. 2007. Neuroprotection from secondary injury by polyethylene glycol requires its internalization. J Exp Biol 210:1455–1462.

Liu Y, Miyoshi H, Nakamura M. 2007. Novel drug delivery system of hollow mesoporous silica nanocapsules with thin shells: preparation and fluorescein isothiocyanate (FITC) release kinetics. Colloids Surf B Biointerfaces 58:180–187.

Luo J, Shi R. 2004. Acrolein induces axolemmal disruption, oxidative stress, and mitochondrial impairment in spinal cord tissue. Neurochem Int 44:475–486.

Luo J, Shi R. 2005. Acrolein induces oxidative stress in brain mitochondria. Neurochem Int 46:243–252.

Luo J, Borgens RB, Shi R. 2002. Polyethylene glycol immediately repairs neuronal membranes and inhibits free radical production after acute spinal cord injury. J Neurochem 83:471–480.

Luo J, Borgens R, Shi R. 2004. Polyethylene glycol improves function and reduces oxidative stress in synaptosomal preparations following spinal cord injury. J Neurotrauma 21:994–1007.

Luo J, Robinson JP, Shi R. 2005. Acrolein-induced cell death in PC12 cells: role of mitochondria-mediated oxidative stress. Neurochem Int 47:449–457.

Marks JD, Pan CY, Bushell T, Cromie W, Lee RC. 2001. Amphiphilic, tri-block copolymers provide potent membrane-targeted neuroprotection. FASEB J 15:1107–1109.

Mohanraj VJ, Chen Y. 2006. Nanoparticles—a review. Trop J Pharm Res 5:561–573.

Nakajima N, Ikada Y. 1994. Fusogenic activity of various water-soluble polymers. J Biomaterials Sci Polymer Ed 6:751–759.

Pathak S, Cao E, Davidson MC, Jin S, Silva GA. 2006. Quantum dot applications to neuroscience: new tools for probing neurons and glia. J Neurosci 26:1893–1895.

Santra S, Zhang P, Wang K, Tapec R, Tan W. 2001. Conjugation of biomolecules with luminophore-doped silica nanoparticles for photostable biomarkers. Anal Chem 73:4988–4993.

Shi R, Borgens RB. 1999a. Acute repair of crushed guinea pig spinal cord by polyethylene glycol. J Neurophysiol 81:2406–2414.

Shi R, Borgens RB. 1999b. Polyethylene glycol repairs mammalian spinal cord axons after compression injury: a morphological study. J Neurotrauma 16:1014.

Shi R, Borgens RB. 2000. Anatomical repair of nerve membranes in crushed mammalian spinal cord with polyethylene glycol. J Neurocytol 29:633–643.

Shi R, Pryor JD. 2000a. Characteristics of action potential conductance failure following stretch injury of isolated mammalian spinal cord. Soc Neurosci Abstr 26:1834.

Shi R, Pryor JD. 2000b. Temperature dependence of membrane sealing following transection in mammalian spinal cord axons. Neuroscince 98:157–166.

Shi R, Luo J, Peasley MA. 2002. Acrolein inflicts axonal membrane disruption and conduction loss in isolated guinea pig spinal cord. Neuroscience 115:337–340.

Silva GA. 2006. Neuroscience nanotechnology: progress, opportunities and challenges. Nat Rev Neurosci 7:65–74.

Silva GA. 2007. Nanotechnology approaches for drug and small molecule delivery across the blood–brain barrier. Surg Neurol 67:113–116.

Thuret S, Moon LD, Gage FH. 2006. Therapeutic interventions after spinal cord injury. Nat Rev Neurosci 7:628–643.

Wang L, Wang K, Santra S, Zhao X, Hilliard LR, Smith JE, Wu Y, Tan W. 2006. Watching silica nanoparticles glow in the biological world. Anal Chem, p 647–654.

Working P, Newman M, Johnson J, Cornacoff J. 1997. Safety of polyethylene glycol and polyethylene glycol derivatives. In: Milton Harris J, Zalipsky S, editors. Poly(ethylene glycol) chemistry and biological applications. Washington, DC: American Chemistry Society. p 45–47.

Xu YH, Bai J, Wang J-P. 2007. High-magnetic-moment multifunctional nanoparticles for nanomedicine applications. J Magnet Magnet Materials 311:131–134.

Yan J, Estevez MC, Smith JE, Wang KK, He X, Wang L, Tan W. 2007. Dye-doped nanoparticles for bioanlysis. Nanotoday 2:44–50.

Zhao XJ, Bagwe RP, Tan WH. 2004. Development of organic-dye-doped silica nanoparticles in a reverse microemulsion. Adv Materials 16:173–176.